

Breakthrough studies and mass transfer studies on the decolorization of paint industry wastewater using encapsulated beads of *Cactus opuntia* (*ficus-indica*)

S. Vishali^{a,*}, P. Mullai^b, R. Karthikeyan^c

^aDepartment of Chemical Engineering, SRMIST, Kattankulathur – 603 203, Tamil Nadu, India, Tel. +91-94438 83562; email: meet.vishali@gmail.com

^bDepartment of Chemical Engineering, Annamalai University, Chidambaram 608 002, India, Tel. +91-94869 18357; email: pmullai@yahoo.in

^cAnjalai Ammal Mahalingham Engineering College, Thanjavur – 614 403, Tamil Nadu, India, Tel. +91-99405 61915; email: drrkarthi@yahoo.com

Received 3 April 2019; Accepted 14 September 2019

ABSTRACT

This article reports the performance of an encapsulated form of *C. opuntia* as an adsorbent for the decolorization of water-based paint industry wastewater in a fixed-bed column. Experimental results revealed that the performance is excellent under these conditions. The impact of operational variables viz., adsorbent bed height, effluent flow rate and effluent initial concentration, on the breakthrough curves was analyzed. Breakthrough curves were validated with the help of different models viz., Thomas/Bed depth service time, Adams–Bohart, Yoon–Nelson and Wang. To identify the rate limiting step of the process, various mass transfer models such as Weber–Morris, Boyd, Úrano–Tachikawa, and Mathews–Weber were performed. From the model parameters, it was concluded that the intra particle diffusion was not the only rate controlling step but film diffusion was also a likely influencing factor. The results recommended that the green-based encapsulated adsorbent *C. opuntia* guaranteed its ability to act as an adsorbent in the decolorization of paint industry wastewaters.

Keywords: Paint industry wastewater; *C. opuntia*; Immobilized beads; Breakthrough curves; Mass transfer studies

1. Introduction

A developing country such as India has plenty of opportunities in the growth of paint industry, the boom in the infrastructure development aided by the easy availability of housing loans is the prime driving force for the growth of the decorative paint segment. The industrial paints sector is witnessing a 50% increase in revenue, mainly due to a 10% rise in the manufacture of automobiles. So the expected paint industry effluent generation is also in the increasing trend [1]. The paint effluent has to be treated before disposal, due to its hazardous composition such as the presence of heavy metals and high concentration of organic matter, which endanger aquatic life and wildlife and contaminate the food

chain. It is the responsibility of the individual to safeguard the quality of the environment.

The treated wastewater can be effectively, recycled and reused within the plant as a coolant, diluent or a component of low-cost paint, and for effective water management. Many physico-chemical methods are tried on the treatment of paint industry effluent, but always biosorption validates its ability in the removal of color and heavy metals [2]. The biosorption process has various merits viz., thorough pollutant removal from dilute solutions, simple and easy operation and it becomes cheaper, when the selected adsorbent does not need any additional pre-treatment process. If the selected adsorbent is either a natural product or an

* Corresponding author.

industrial waste, the treatment will be done in a more economical way. The preparation of new and effective low-cost adsorbent is extremely essential for the treatment of paint effluent. From the literature, it was noticed that, *S. potatorum*, *Moringa oleifera*, Guar gum and Crab shell wastes were attempted as an adsorbent in the treatment of paint industry effluent and proved its ability in the decolorization [3].

The literature suggested the new eco-friendly adsorbent for the treatment of paint industry effluent. *Cactus opuntia (ficus-indica)* commonly known as prickly pear, which grows well in dry land and the availability was found in United States, Mexico, South America and other areas including Africa, Australia and Mediterranean regions [4]. The hetero polysaccharide is a component which has $2.3\text{--}300 \times 10^4$ g/mol of molecular weight and is a primary constituent of cactus cladode. It was used as a coagulant in the treatment of paint industry wastewater [5], turbidity removal from surface water and wastewater [6–8]. The adsorption capacity of Cactus has been tested in the removal of cadmium and lead, chromium (VI) [9], Pb^{2+} [10] and in the removal of Methylene blue, Eriochrome Black, Alizarin S [4] and brilliant green dyes [11]. As an added application, it is used as thickener, emulsifier in food industry and also has utilization in cosmetic industry. There is no information in literature of utilizing cactus as an adsorbent for the treatment of paint effluent.

This work is focused onto the evaluation of the performance of *C. opuntia* as an encapsulated adsorbent for the decolorization of water-based paint industry wastewater (WPW) in a fixed-bed column. The influence of the design parameters in the breakthrough curves was analyzed.

2. Materials and methods

2.1. Materials

2.1.1. Wastewater

All chemicals used in the study were of analytical grade (AR). The WPW was synthetically produced by adding white primer and colorant (5% v/v) using double distilled water. Three samples with different initial concentration viz., 3,100; 5,650 and 7,693 mg/L were prepared and labeled as Sample numbers 1–3, respectively (Table 1). The physico-chemical characteristics of the effluent were analyzed and the results are given in Table 2 [12].

2.1.2. Adsorbent

Pads of *C. opuntia* were collected from Thirumayam, an agronomic area of Pudukottai district, South India.

Table 1
Concentration of WPW (made up to 1,000 mL)

Sample number	White primer (mL)	Blue colorant (mL)	Initial COD (mg/L)
1	48	2	3,100
2	44	6	5,650
3	40	10	7,693

Table 2
Physico-chemical characteristics of the WPW (Sample number 3) [12]

Parameters	Concentration (except for pH, color and turbidity)
pH at 25°C	7.6
Color, nm	0.4583
Total dissolved solids, mg/L	304
Total suspended solids, mg/L	6,880
Oil and grease, mg/L	19
Chloride as Cl, mg/L	68
Chemical oxygen demand (COD), mg/L	7,693
Sulfate as SO_4 , mg/L	24
Biochemical oxygen demand, mg/L (5 d) incubated at 27°C	2,648
Iron as Fe, mg/L	0.05
Turbidity, NTU	7,760

The thorns present in the pads were completely removed before washing thoroughly with distilled water, after which the pads were sliced into small pieces, and dried in a convection oven at 100°C for 1 h with periodical supervision. The dried material was powdered using conventional mixer and sieved through a 0.5 mm sieve (Fig. 1).

2.1.3. Fixed-bed column

A fixed-bed column (FBC) was fabricated with a 2 cm inner diameter and a 50 cm length with tapered end using Pyrex glass (Fig. 2). The wastewater was passed into an FBC from the top using a peristaltic pump (Ravel Hiteks, India) with controlled flow rate at room temperature (30°C).

2.2. Methods

2.2.1. Preparation of encapsulated beads

With the help of the sodium alginate component, the encapsulation of *C. opuntia* was done. The *C. opuntia* powder (3% (w/v)) and sodium alginate (1% (w/v)) was suspended in distilled water utilizing magnetic stirrer with hot plate. In order to ensure the homogenous mixing without any lumps, warm temperature was maintained ($\leq 45^\circ\text{C}$). The adsorbent may lose its properties when the temperature was raised. The resultant mixture was expelled as a drop in sterile 3% CaCl_2 solution at room temperature, using a syringe. The encapsulated beads were hardened by re-suspending in a fresh CaCl_2 solution for 24 h at 4°C and finally these beads were washed with de-ionized water to remove excess calcium ions. Encapsulated beads were prepared using sodium alginate alone and used as a control [2].

2.2.2. Experimental set-up

At the bottom of a fixed-bed column (FBC) glass wool and above that glass beads were placed. The glass beads were



Fig. 1. *C. opuntia* pads, powder and immobilized beads.

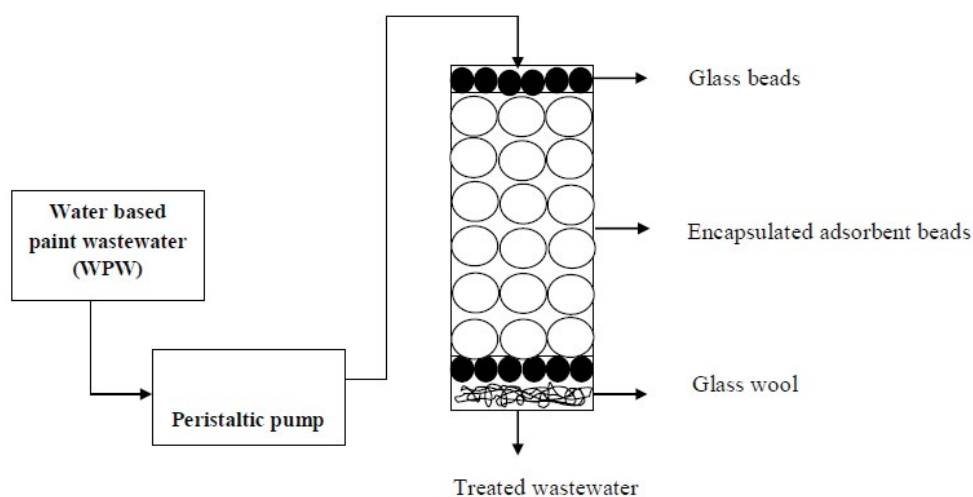


Fig. 2. A fixed-bed column.

acting as a supporting layer and glass wool was placed to avoid the blockage of glass beads in the outlet. The encapsulated beads of *C. opuntia* were packed in the column to the desired height, between two supporting layers of glass beads. The presence of glass beads at the top is to provide a uniform inlet flow. In a down flow mode, the adsorbate was introduced, at a controlled flow rate and at a room temperature of 30°C without any pH adjustment.

As a first step of the packing of the beads, distilled water was half filled in a fixed-bed column, then a known mass of beads were gently added. Due to the concept of terminal settling velocity, close to constant and uniform packing was achieved for each run. The water was drained out, after the acquirement of desired bed height, which resulted in more compressed packing. At regular spell, the treated wastewater was collected for residual color analysis.

The treatment was terminated once the column has reached the saturation point. To ensure the reproducibility, the experiments were performed thrice. The reported values were the average of three data sets. The experiments were repeated to understand the impact of bed height, flow rate and initial concentration of WPW on removal efficiency.

2.2.3. Analysis

The ability of the adsorbent in the WPW treatment was analyzed in terms of residual color at λ_{\max} 612 nm in a SL 218 double UV visible spectrophotometer (Elico, India). The λ_{\max} was selected by scanning the sample between 200 and 800 nm and the peak was observed at 612 nm.

3. Design parameters of adsorption column

Fixed-bed column (FBC) experiments are performed to generate data that will enable the record of breakthrough curves. The breakthrough time and the shape of the breakthrough curve are very important determinants of the dynamic response of the adsorption column. The breakthrough time is defined as the time of adsorption when the outlet concentration from the column is about 5%–10% of the inlet concentration. The depth of the exchange zone, time required for the exchange zone to move its own height, adsorption rate and adsorption capacity are some of the main considerations when designing an adsorption column [13]. They are generally expressed in terms of normalized dye

concentration, defined as the ratio of instantaneous or outlet adsorbate concentration to the initial adsorbate concentration (C_t/C_0), as a function of time for a given bed height or adsorbate flow rate [14].

In the present studies of fixed-bed adsorption process, the adsorption capacities of pollutant at breakthrough (q_b) and exhaustion (q_e) time, the breakthrough time (t_b), time equivalent to the total capacity of column (t_t), the exhaustion time (t_e), the total or stoichiometric amount of solute adsorbed (q_t), the total amount of solute sent to the column (m_t), volume of effluent treated (V_{eff}) and empty bed residence time (EBRT) are usually used in the description and comparison. For a desired bed height, flow rate and initial concentration of WPW, the value of the total mass of solute adsorbed, q_t (mg) can be calculated as being equal to the area under the plot of the adsorbed solute concentration (Table 3).

4. Results and discussions

4.1. Characterization of *C. opuntia* (*ficus-indica*)

The FTIR spectrum of *C. opuntia* is shown in Fig. 3a and the functional groups are listed in Table 4. Using the glucose solution, the existence of cellulose in *C. opuntia* powder was estimated using glucose solution. It was observed from the glucose standard curve that the 1,000 μL of *C. opuntia* eluate contains 91.87 mole of cellulose in it. Energy-dispersive X-ray spectroscopy (EDS), scanning electron microscope (SEM), X-ray diffraction (XRD) is explained in Figs. 3b–d [5].

The mean diameter of the immobilized bead was calculated using volume displacement method and the value

was 0.5186 cm. The bead density (ρ_p) 0.7904 g/cc was calculated by using the ratio between the mass of known number of beads and its volume. The bulk density (ρ_b) of the adsorbent was also calculated using the ratio between the total mass of the beads used for the required packing height per volume of the beads, and the value was 0.8280 g/cc.

4.2. Influence of operating variables on breakthrough curves

4.2.1. Influence of bed height

The term bed height is related with the mass of adsorbent used, which indirectly dictates the availability of active sites on it. The entire adsorption process depends on the availability of the adsorbent dose based on the initial concentration of the pollutant. The scale up of a fixed-bed column to handle a specific load of pollutant present in the WPW may end with unsatisfactory way due to insufficient bed height.

Columns with 10, 15 and 25 cm height prepared from encapsulated *C. opuntia* beads, recorded during 195, 295 and 395 min as time taken to attain saturation. The initial concentration of the effluent (3,100 mg/L [sample number 1]) and flow rate (5 cc/min) were kept constant (Fig. 4). The breakthrough times under these conditions were 185, 280 and 375 min. The total percentage removal of color rose from 75% to 96% when the adsorbent bed height was increased. Following the same trend, adsorption capacities (q_t) were 32, 48 and 57 mg/g, and the length of mass transfer zone advanced from 9.47 to 23.68 cm. Similarly, the volume of treated effluent escalated from 975 to 1,975 mL and the EBRT increased from 6.28 to 15.7 cm (Table 5).

Table 3
Process analysis parameters of a FBC

Volume of effluent treated, mL	$V_{\text{eff}} = Qt_t$
Empty bed residence time (EBRT),min	$\frac{\text{Bedvolume}}{\text{Volumetric flowrate of the effluent}}$
Total quantity of solute adsorbed for a given C_0 , Q , mg	$q_t = QC_0 \int_0^{t_t} \left(1 - \frac{C_t}{C_0}\right) \times dt$
Total amount of solute sent to the column, mg	$\frac{C_0 Qt_t}{1,000}$
Exhaustion rate of adsorbent	$\frac{\text{mass of adsorbent in column}}{\text{Volume treated at B.T}}$
Total color removal %	$\frac{q_t 1,000}{C_0 Qt_t}$
Total stoichiometric capacity of the column, min	$\frac{q_t t_t}{m_t}$
Mass transfer zone or equivalent length of unused bed (MTZ), cm	$H \left(1 - \frac{t_b}{t_s}\right)$
q_e , mg/g	$\frac{q_t}{m}$

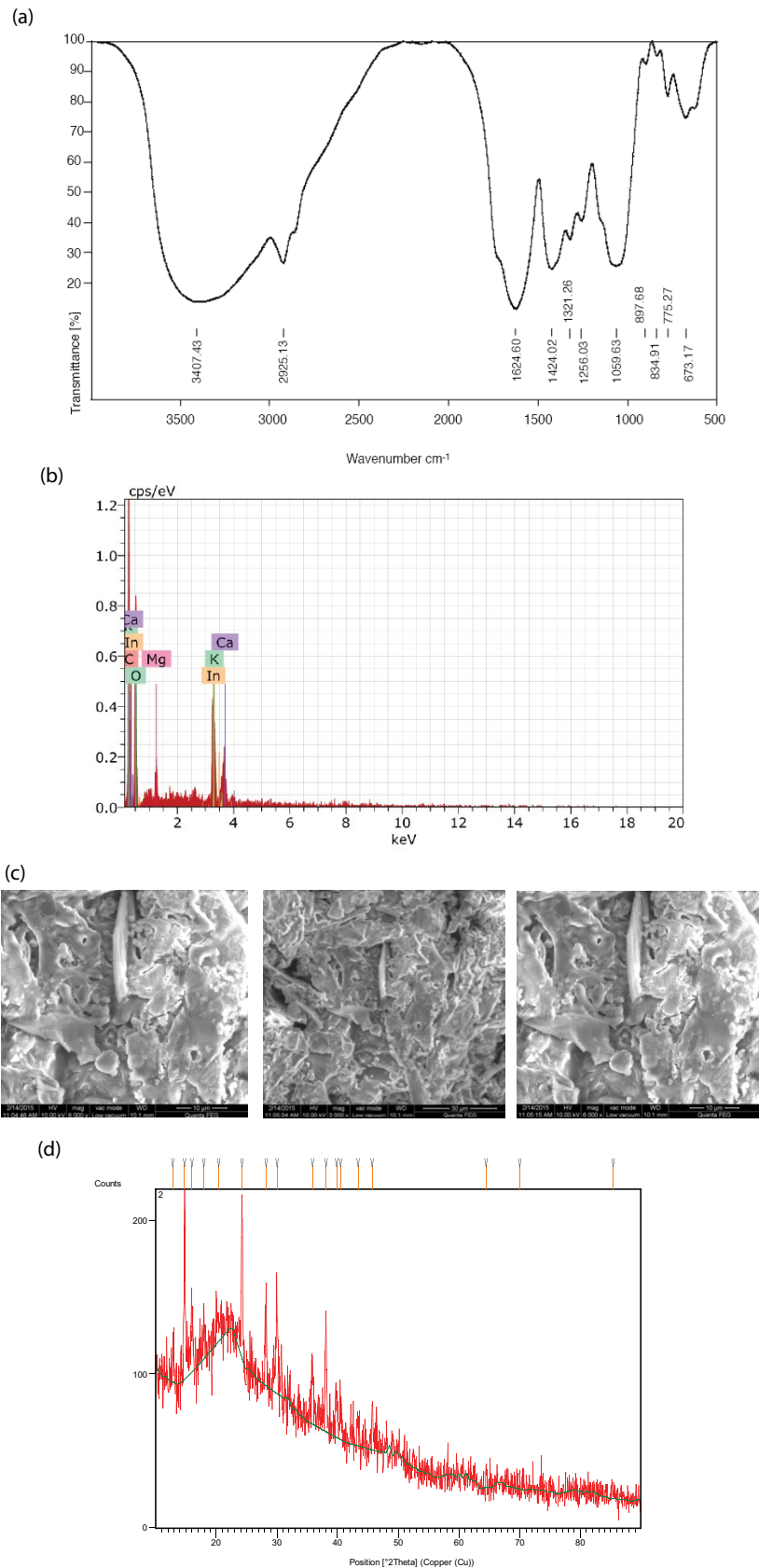


Fig. 3. (a) Fourier transform infrared spectroscopy (FTIR) spectrum of *C. opuntia (ficus-indica)*. (b) Elemental analysis of *C. opuntia (ficus-indica)* using energy-dispersive X-ray spectroscopy (EDS). (c) Scanning electron microscope (SEM) image of *C. opuntia (ficus-indica)*. (d) X-ray diffraction (XRD) of *C. opuntia (ficus-indica)*.

Table 4
FTIR characterization of *C. opuntia (ficus-indica)* [5]

Wavelength (cm ⁻¹)	Nature	Functional group
3,405.43	Strong peak	Polymeric OH stretching vibration of water and stretching vibration of amine
3,000	Peak	Presence of C=C–H group, which indicates aromatic ring
1,500	Sharp Peak	Presence of benzene group
1,424.02	Peak	Presence of carboxylic acid salt
1,321.26	Peak	Aromatic primary amine stretch, CN stretch
1,624.3	Peak	C=C stretch
From 897 to 673	Several peaks	Aromatic group

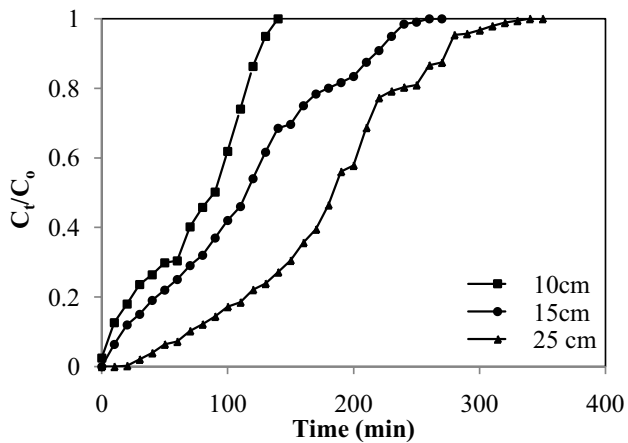


Fig. 4. Influence of bed height on color removal in a FBC. Bed height: 5–25 cm; Flow rate: 5 cc/min; initial concentration: 3,100 mg/L.

Furthermore, the slope of the breakthrough curve became flatter as the bed height went up, thereby giving rise to a broadened mass transfer zone. The slope of the breakthrough curve decreased with the increase of bed height, probably because of the increase of contact time of adsorbate with the adsorbent, which in turn improved the removal capacity

Table 5
Influence of operating variables on a FBC design parameters

C_0	Q	H	t_t	q_t	t_b	t_s	V_{eff}	EBRT	Total color removal	MTZ
mg/L	cc/min	cm	min	mg/g	min	Min	mL	min	%	cm
3,100	5	10	195	32	185	10	975	6.28	75	9.47
3,100	5	15	295	48	280	15	1,475	9.42	89	14.21
3,100	5	25	395	57	375	20	1,975	15.7	96	23.68
3,100	10	25	345	55	328	17	3,450	7.9	53	23.68
3,100	15	25	295	55	280	15	4,425	5.2	41	23.68
5,650	5	25	270	118	257	14	1,350	15.7	82	23.68
7,693	5	25	195	133	185	10	975	15.7	77	23.68

and lowered solute concentration in the effluent. Identical outcomes were observed when the textile dye direct blue 86 was decolorized using a composite adsorbent [15].

4.2.2. Influence of flow rate

The total time taken to conduct each run showed a downward trend as flow rate stepped up from 5 to 15 cc/min. Figures for total time and breakthrough time were 395, 345 and 295 min and 375, 328 and 280 min for flow rate values of 5, 10 and 15 mL/min, respectively. Steeper and faster breakthrough curves emerged with faster flow rate. The total percentage of color removal corresponding to the stoichiometric capacity of the column was found to diminish from 96% to 41% with an elevation in the flow rate (Fig. 5). Adsorption capacity recorded a fall from 57 to 55 mg/g, while EBRT came down from 15.7 to 5.2 min. The total volume of the treated effluent increased from 1,975 to 4,425 mL. The mass transfer zone size was maintained constant at 23.68 cm.

The uptake of pollutant (color) was maximum in the initial stages and became gradually lower, and finally the adsorbent reached the saturation point. Lowering of the flow rate prolonged contact time but narrowed down the adsorption zone. When the volumetric flow rate altered from 5 to 15 cc/min, the breakthrough curves became steeper and reached the breakthrough point in a shorter period. This may

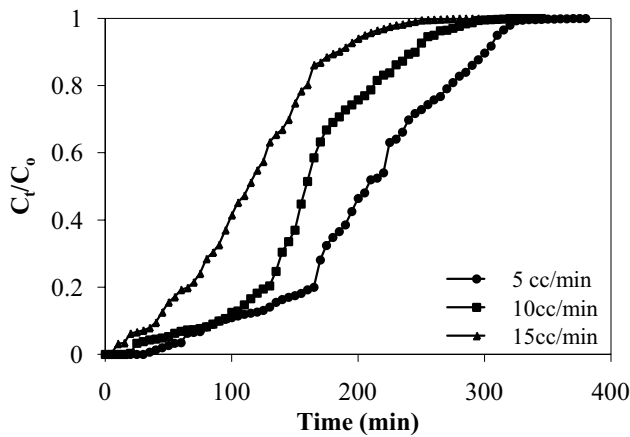


Fig. 5. Influence of flow rate on color removal in a FBC. Bed height: 5 cm; flow rate: 5–15 cc/min; initial concentration: 3,100 mg/L.

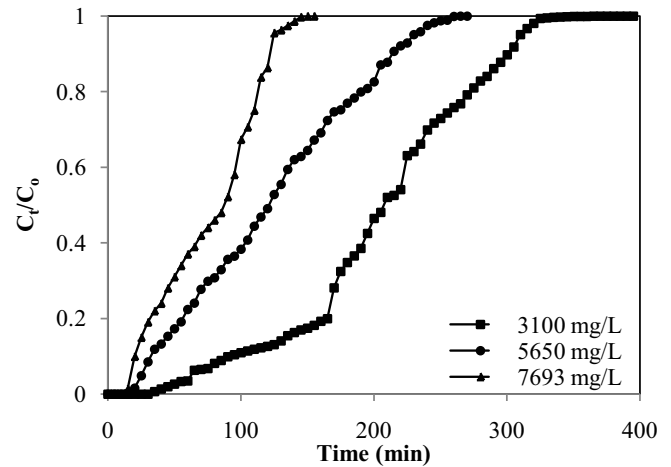


Fig. 6. Influence of initial concentration on color removal in a FBC. Bed height: 25 cm; flow rate: 5 cc/min; initial concentration: 3,100–7,693 mg/L.

be because (a) the increase in pollutant load resulted with rapid saturation and (b) the decrease in the adsorbate residence time in the column prevents the diffusion of adsorbate on the adsorbent pores. The contact time between pollutant and adsorbent was very brief at higher flow rates, resulting in a fall of removal efficiency (Table 4) [16].

To sum up, it can be said with certainty that at a higher linear flow rate, the adsorbent got saturated quickly, because of higher pollutant load and shorter contact time. The results were coincided with the removal of Cu^{2+} from solution using rice husk as in adsorbent [17].

4.2.3. Influence of effluent initial concentration

The effect of initial WPW concentration was investigated by varying its concentration as 3,100; 5,650 and 7,693 mg/L with adsorbent bed height and flow rate of 25 cm and 5 cc/min, respectively. According to Fig. 6, higher levels of initial effluent concentration (from 3,100 to 7,693 mg/L), brought down breakthrough time from 375 to 185 min (Table 4). The other parameters that were decreased included total time, corresponding to stoichiometric capacity of the column (from 395 to 195 min.), volume of treated water (1,975; 1,350 and 975 mL), and total percentage removal of color for a FBC (96%, 82% and 77%). It is evident from the plots that the adsorbent beds were exhausted faster at higher adsorbate inlet concentration, which was 7,693 mg/L. The EBRT and mass transfer zone were steady at 15.7 min and 23.68 cm, respectively, whereas the equilibrium adsorption uptake went up (57, 118 and 185 mg/g) (Table 4).

It was observed that the adsorption site of the adsorbent was saturated quickly while treating the effluent with higher initial concentration. The breakthrough time was shorter in case of higher initial concentration and higher for effluent with lower initial concentration. Using this given system, higher volume of lower initial concentration effluent could be treated. Similar to the results of the current study, it was viewed in the breakthrough curve analysis of Mn(II) ions from wastewater by using *Mangostana garcinia* peel-based granular activated carbon also [18].

4.3. Modeling of breakthrough curves

The shape of the breakthrough curve and time or bed volume for breakthrough appearance are crucial for determining the operational and dynamic response of an adsorption column. Furthermore, successful design of an adsorption column rests on the accurate prediction of the concentration–time profile from the breakthrough curve for the discharge of specific effluents from a column. With a view to throw light on the adsorption process of color from WPW, several models were applied to study adsorption breakthrough curves using encapsulated *C. opuntia* [19].

Systematic analysis of a fixed-bed column (FBC) experiments for the process of color adsorption and prediction of the breakthrough curve necessitated the employment of several theoretical models, such as Thomas or bed depth service time (BDST) model, Adams–Bohart model, Yoon–Nelson model and Wang model. The linearized form of all the breakthrough models is given in Table 6 [20].

4.3.1. Evaluation of Thomas model parameters

From the slope and intercept of the linear Thomas model (Fig. 7a), drawn with $\ln(C_t/(C_0 - C_t))$ vs. time, it was demonstrated that the model rate constant k_{BDST} and the adsorption capacity q_{BDST} were dependent on flow rate, bed height and initial concentration of adsorbate. A high regression coefficient (R^2) value indicated that the kinetic data conformed well to the Thomas model.

When *C. opuntia* was used as an immobilized bead, the model rate constant k_{Th} decreased (0.0942 to 0.0798 L/min mg, 0.0995 to 0.0223 L/min mg), with the increase in bed height and initial effluent concentration, respectively. The constant increased in value from 0.0995 to 0.1205 L/min mg, with higher flow rate. With regard to the readings for q_{BDST} (mg/g), maximum adsorption capacity took a downward slide from 9.83 to 4.38 mg/g with a gradual upgradation of bed height from 10 to 25 cm. A faster flow rate and initial concentration, respectively, resulted in enhanced adsorption capacity thus: 4.38 to 7.79 and 4.38 to 15.42 mg/g, respectively. High

Table 6
Breakthrough curve models for a FBC

BDST	$\ln \left[\left(\frac{C_0}{C_t} \right) - 1 \right] = (-k_{\text{BDST}} C_0) t + \frac{k_{\text{BDST}} q_{\text{BDST}} m}{Q}$
Adams–Bohart	$\ln \left(\frac{C_t}{C_0} \right) = (k_{\text{AB}} C_0) t - \frac{k_{\text{AB}} N_0 H}{U_0}$
Yoon–Nelson model	$\ln \left(\frac{C_t}{C_0 - C_t} \right) = k_{\text{YN}} t - k_{\text{YN}} \tau$
Wang	$\ln \left[\frac{1}{1} - \left(\frac{C_t}{C_0} \right) \right] = -k_w t + k_w t_{0.5}$

regression coefficient values confirmed that the kinetic data fitted well with the Thomas model (Table 7). The kinetic constant k_{TH} went up with an increase in flow rate, but came down when bed height and initial concentration were raised [18].

4.3.2. Evaluation of Adams–Bohart model parameters

The mass transfer coefficient (k_{AB}) and maximum adsorption capacity (N_0) values were calculated from the slope and intercept of the linear curves (Fig. 7b), respectively, and listed in Table 7.

An increase in bed height and flow rate resulted in a rise in k_{AB} values; the reverse was noticed for initial concentration. With an increase in bed height and flow rate, N_0 came down (8.85, 7.64, 5.97 mg/L) and went up (5.97, 10.44 and 12.79 mg/L), respectively. In the case of initial concentration, N_0 shot up (5.97, 35.1, 61.07 mg/L). The linear regression coefficient R^2 ranged from 0.649 to 0.942.

The adsorbent displayed a gradual downward slant in their adsorption capacity with augmented flow rate of effluent. The elevated initial concentration enhanced the maximum adsorption capacity per unit volume of adsorption column or N_0 (mg/L). The driving force behind adsorption was the concentration difference between the

pollutant on the surface of the adsorbent and in the effluent. The concentration gradient increased with initial concentration. This demonstrated that the overall system kinetics was dominated by external mass transfer in the initial part of adsorption in the column [21].

4.3.3. Evaluation of Yoon–Nelson model parameters

The Yoon and Nelson equation regarding a single-component system was investigated where k_{YN} the rate constant (l/min), τ is the time required for 50% adsorbate breakthrough (min), and t is the breakthrough (sampling) time (min). A plot of $\ln [C_t/(C_0 - C_t)]$ vs. t gave a straight line with slope of k_{YN} and intercept of $-\tau$ (Fig. 7c).

The k_{YN} value declined from 0.028 to 0.024 min⁻¹ and the τ value heightened from 79 to 189 min when bed height grew from 10 to 25 cm. With faster flow rate, the k_{YN} upturned and τ value shrank from 189 to 112 min. There was a marked influence of initial concentration on both k_{YN} and τ . k_{YN} climbed and τ value reduced (Table 7). The maximum value of R^2 was 0.963.

The time required for 50% breakthrough τ reduced with elevation of both flow rate and initial ion concentration. High values of correlation coefficients indicated that the Yoon and Nelson model fitted well with the experimental

Table 7
Parameters of breakthrough models in an FBC at various conditions

C_0	Q	H	BDST			Adams–Bohart			Yoon–Nelson			Wang		
			k_{BDST}	q_{BDST}	R^2	k_{AB}	N_0	R^2	k_{YN}	τ	R^2	k_w	$t_{0.5}$	R^2
mg/L	cc/min	cm	L/(min mg)	mg/g		L/(min mg)	mg/L		l/min	min		l/min	min	
3,100	5	10	0.0942	9.83	0.662	0.0273	8.85	0.771	0.028	79	0.662	0.0189	30	0.568
3,100	5	15	0.0798	5.66	0.819	0.0330	7.64	0.563	0.024	136	0.819	0.0121	47	0.696
3,100	5	25	0.0995	4.38	0.909	0.0376	5.97	0.866	0.030	189	0.909	0.0155	92	0.650
3,100	10	25	0.1065	7.24	0.963	0.0399	10.44	0.808	0.032	157	0.963	0.0169	72	0.778
3,100	15	25	0.1205	7.79	0.961	0.0393	12.79	0.649	0.036	112	0.962	0.0226	54	0.857
5,650	5	25	0.0299	7.62	0.948	0.0128	35.10	0.766	0.028	119	0.919	0.0160	50	0.752
7,693	5	25	0.0223	15.42	0.895	0.0111	61.07	0.942	0.042	111	0.873	0.0193	47	0.594

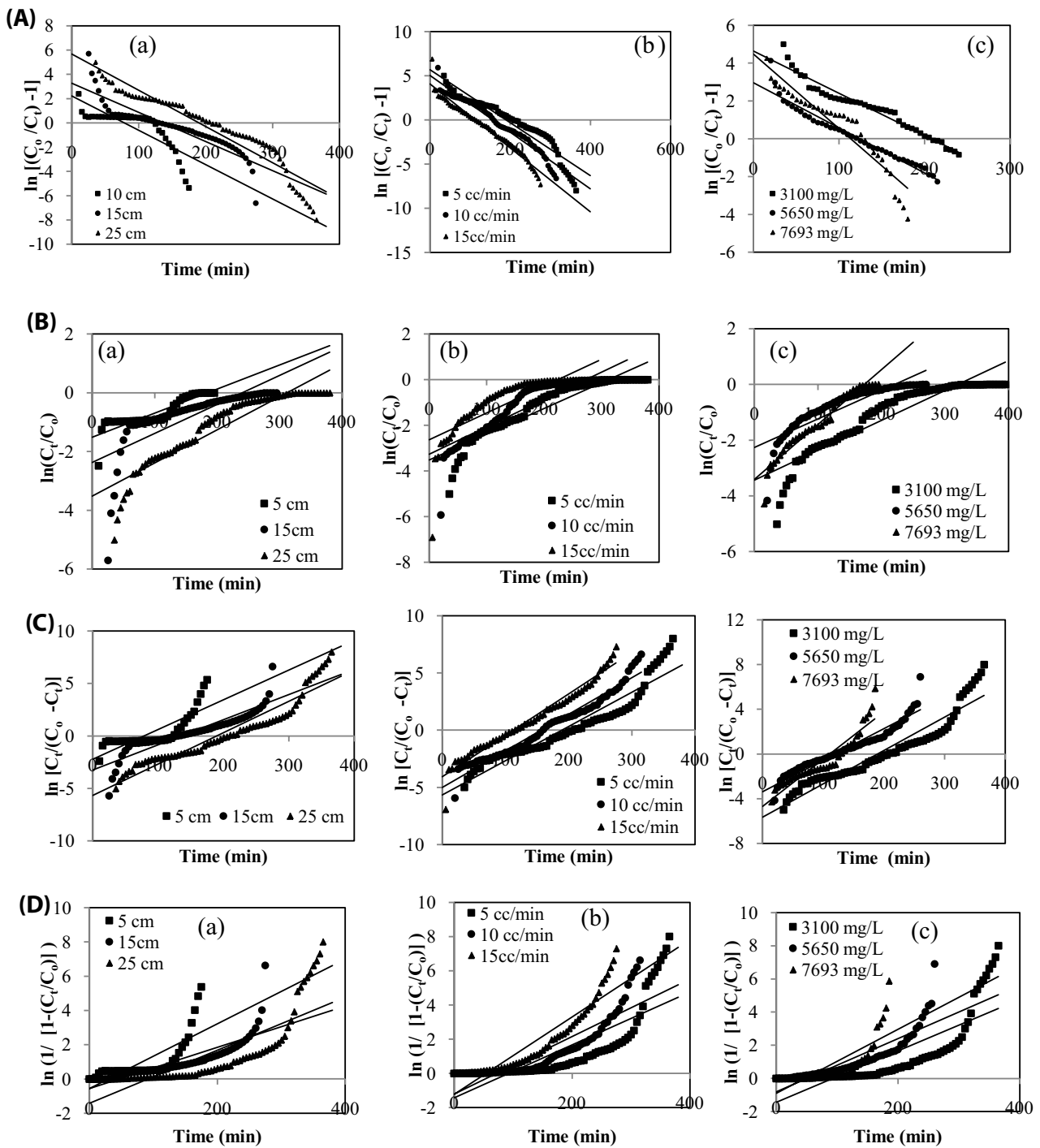


Fig. 7. (A) BDST model: (a) bed height, (b) flow rate, (c) initial concentration. (B) Adams–Bohart model: (a) bed height, (b) flow rate, (c) initial concentration. (C) Yoon–Nelson model: (a) bed height, (b) flow rate, (c) initial concentration. (D) Wang model: (a) bed height, (b) flow rate, (c) initial concentration.

data. It was also found that the rate constant (k_{YN}) increased in parallel with increase in flow rate. As a result of lowered residence time of pollutants in the adsorbent bed, the time required for 50% adsorbate breakthrough (τ) came down with a rise in flow rate. A larger residence time of adsorbate within the column caused the τ value to elapse with a rise in the bed height [21].

4.3.4. Evaluation of Wang model parameters

A plot of $\ln[1/(1-(C_t/C_0))]$ vs. t (Fig. 7d) produces the slope and intercept value as $1/k_w$ and $t_{0.5}$, respectively, where k_w is the kinetic constant and $t_{0.5}$ time required for 50% adsorbate breakthrough time (min) (Table 7).

Greater bed height affected a rise in $t_{0.5}$ from 30 to 92 min but this value showed a downward trend (92, 72 and 54 min) with a more rapid flow rate. The Wang model rate constant came down with a rise in bed height, but went up with increase in flow rate and initial concentration, respectively.

The time required for 50% breakthrough $t_{0.5}$ shortened with both faster flow rate and intensified initial ion concentration. The reason for such behavior was that slower flow rate ensured longer contact time with a resultant higher breakthrough time. The large amount of pollutant in terms of initial concentration took much time, to decolorize and reach 50% of its original quantity. The larger residence time of adsorbate within the column caused the $t_{0.5}$ value to elapse with a greater bed height.

4.4. Mass transfer studies in a fixed-bed column

The linearized forms of mass transfer models are listed in Table 8 and the model parameters are listed in Table 9.

4.4.1. Application of Weber–Morris model

k_{WM} was the intra particle diffusion rate constant which showed a reduction with increase in bed height. It became higher along with flow rate. With initial concentration, the

values were also elevated. The linear regression coefficient ranged between 0.4154 and 0.8629. It can be seen from the small value of the intra particle diffusion constant that the boundary layer has less significant effect on the diffusion mechanism of pollutant uptake by the adsorbents [22].

During the process of adsorption, in addition to being adsorbed onto the surface of the adsorbent, mass transfer may also take place due to intra particle diffusion. In such a situation, the plot will not pass through the origin, indicating that the intra particle diffusion was not the singular rate controlling step, and that film diffusion should not be ruled out as a possible rate controlling factor. In the present study, large k_{WM} values pointed to easier diffusion and transport into the pores of the adsorbents. The value of intercept I gave an idea about the boundary layer thickness: the larger the intercept the greater is the boundary layer effect. The observed large intercept also indicated that the effects on mass transfer resistance on the adsorbate were gradually higher, thereby suggesting that external mass transfer resistance could not be ignored.

From Fig. 8a the non-linearity of the points explains that more than one process determined the adsorption. The interception of the two lines indicated that the treatment is done by (i) an external diffusion mechanism, (ii) intra particle diffusion [23–25].

Table 8
Mass transfer models for a FBC

Weber-Morris	$q_t = k_{WM}t^{0.5} + I$
Boyd	$0.4977 + \ln\left(1 - \frac{q_t}{q_e}\right) = -Bt$; Where $B = \frac{\pi^2 D_i}{r^2}$
Urano-Tachikawa	$\log\left(1 - \left(\frac{q_t}{q_e}\right)^2\right) = \left(\frac{-4\pi^2 D_{UT}}{2.3d^2}\right)t$
Mathews-Weber	$\ln\left(\frac{C_t}{C_0}\right) = \left(-k_{MW} \frac{q}{V}\right)t$; where $\frac{a}{V} = \frac{6m}{\rho_p d}$

Table 9
Parameters of mass transfer models in an FBC at various conditions

C_0	Q	H	Weber–Morris	Boyd	Urano–Tachikawa	Mathews-Weber
			k_{WM}	D_i	D_{UT}	k_{MW}
mg/L	cc/min	cm	mg/(min ^{0.5} g)	cm ² /min	cm ² /min	cm/min
3,100	5	5	0.0922	7.57E -05	7.68E-05	1.88E-05
3,100	5	15	0.0772	4.64E-05	4.55E-05	3.80E-06
3,100	5	25	0.0618	5.46E-05	5.49E-05	2.52E-06
3,100	10	25	0.0720	6.27E-05	6.27E-05	2.84E-06
3,100	15	25	0.0874	9.55E-05	9.25E-05	1.89E-06
5,650	5	25	0.2166	6.14E-05	6.12E-05	2.52E-06
7,693	5	25	0.3835	6.27E-05	6.74E-05	7.46E-06

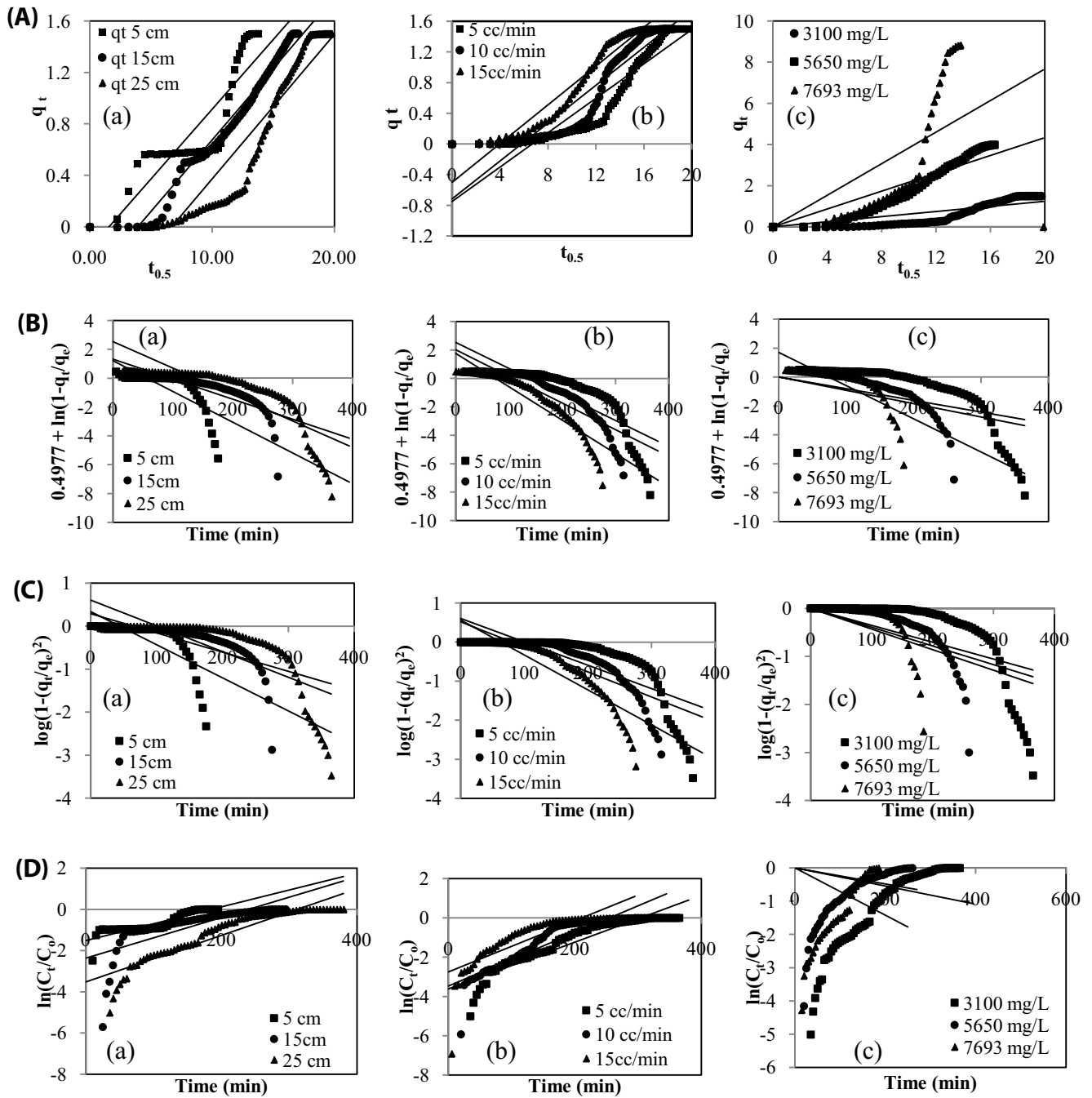


Fig. 8. (A) Weber–Morris model: (a) bed height, (b) flow rate, (c) initial concentration. (B) Boyd model: (a) bed height, (b) flow rate, (c) initial concentration. (C) Urano–Tachikawa model: (a) bed height, (b) flow rate, (c) initial concentration. (D) Mathews–Weber model: (a) bed height, (b) flow rate, (c) initial concentration.

4.4.2. Application of Boyd's model

To demonstrate the slow steps involved in the adsorption process, the kinetics data were also subjected to Boyd kinetics model analysis. The plot of B_t against time showed that the points were scattered and did not pass through the origin (Fig. 8b).

D_i values emerged as 4.64×10^{-5} , 5.46×10^{-5} and 7.57×10^{-5} under the influence of bed height. The diffusion coefficient

showed increments with the speeding up of flow rate. Increase in initial concentration produced sequentially higher D_i figures.

The presence of an intercept showed that diffusion was not the only observed mechanism of transfer. A linear plot, with its slope equal to B , would mean that pore diffusion is the rate controlling step. The effective diffusion coefficient, D_i (cm^2/s), was calculated from this. The observance of an

intercept is predictive of a second mass transfer mechanism (external mass transfer) [25].

4.4.3. Application of Urano–Tachikawa model

The dependence of $f(q_t/q_e)$ on t is plotted in a linear form (Fig. 8c). The constant of the internal diffusion was determined from the slopes of the lines. It was observed that diffusivity showed an upward trend with increase in flow rate and initial concentration. The values ranged from $5.49\text{--}9.25 \times 10^{-5}$ and $5.49\text{--}6.74 \times 10^{-5}$ for flow rate and initial concentration, respectively.

The dependence of $f(q_t/q_e)$ on t is linear within the time interval from 0 to 90 min, except for the small spells of sorption. A deviation from the linear dependence is also seen from the graphical depiction in, where the linear sections do not pass through the origin [26].

When the effluent flow rate increases, the sorbate diffusivity into the adsorbent also increases. The amount of pollutant present in the effluent was directly proportional to its initial concentration. Due to the escalated concentration gradient, with the increase in the initial concentration, the diffusivity also elevated. Earlier studies [27] explained that the DUT values in the range of $10^{-12}\text{--}10^{-13}$ cm²/s confirm that the intra particle diffusion is the rate-limiting step for the adsorption of organic compounds. In the present study, the DUT values were in the order of 10^{-12} cm²/s. The adsorption process could be best explained by the Urano–Tachikawa equation, indicating the controlling nature of intra particle diffusion.

4.4.4. Application of Mathews–Weber model

The Mathews–Weber model is plotted in Fig. 8d. The kinetic constant of Mathews–Weber models showed an upswing with initial concentration and ranged from 1.89×10^{-6} to 2.84×10^{-6} with bed height.

The k_{MW} values decreased with increments in the initial dye concentrations, indicating that the external mass transfer rate is slower at higher initial dye concentration. The velocity of dye transport from liquid phase to solid phase decreased but the intra particle diffusion increased with increase in the initial dye concentrations [28].

5. Conclusions

During the course of this explorative study, it was found that the natural material *C. opuntia* could be used as an adsorbent in the treatment of WPW, for achieving reduction in color, so that the wastewater discharge would fall within the prescribed regulatory safety limits. The materials were characterized using FTIR, EDS, SEM and XRD for their functional groups, chemical compositions, morphological and phase identification, besides confirming the presence of cellulose in *C. opuntia* in substantial quantities.

The percentage color removal was noticed to improve with raise in bed height and decrease with an ascending nature of flow rate and initial concentration of effluent. The existence of huge number of active sites (due to larger bed height), larger gradient in mass transfer (due to higher effluent initial concentration) and greater residence time (due to lower flow rate) resulted in a higher removal efficiency.

Modeling of breakthrough curves was performed. The results of the model parameters revealed (i) adsorption capacity, (ii) kinetic rate constants and (iii) time required to reduce the 50% adsorbate concentration. Mass transfer models were performed to understand the transportation of pollutant and the rate limiting step.

In summary, it may be stated that *C. opuntia* could be effectively used for the treatment of WPW, by virtue of being biodegradable, it is safe to human health, inexpensive, abundantly available and, last but not the least, efficient in the removal of toxic pollutants from WPW. It was also observed that, these materials could act successfully as an adsorbent and propitious surrogate for chemical activated carbon. The results derived for the synthetic WPW were promising and could be useful to apply on real wastewater too.

Symbols

A	—	Total interfacial area of particle, cm ²
C_o, C_e, C_t	—	Concentration of the solute, at $t = 0$, at equilibrium and time t in the effluent, mg/L
D	—	Mean diameter of immobilized beads, cm
D_i	—	Effective diffusivity, cm ² /min
D_{UT}	—	Diffusion constant in Urano–Tachikawa model, cm ² /min
E	—	Mean free energy of adsorption per molecule of adsorbate, kJ/mol
H	—	Bed height, cm
l	—	Thickness of boundary layer, mg/g
k_{AB}	—	Kinetic constant in the model Adams–Bohart, L/(min mg)
k_{BDST}	—	Kinetic constant in the model BDST, L/(min mg)
kid	—	Kinetic rate constant in the intra particle diffusion model, mg/g min ^{0.5}
k_{MW}	—	External mass transfer coefficient from Mathews–Weber model, cm/min
k_w	—	Kinetic constant in the model Wang, 1/min
k_{WM}	—	Kinetic constant in the model Weber–Morris, mg/(min ^{0.5} g)
k_{YN}	—	Kinetic constant in the model Yoon–Nelson, 1/min
M	—	Total mass of adsorbent, g
n	—	Number of measurements
N_0	—	Maximum adsorption capacity per unit volume of adsorption column, mg/L
p	—	Number of parameters present in the adsorption isotherm model
Q	—	Inlet feed flow rate, mL/min
q_{BDST}	—	Maximum adsorption capacity in BDST model, mg/g
q_t, q_e	—	Total quantity of pollutant adsorbed at time t and at equilibrium, mg/g
r	—	Mean radius of immobilized adsorbent beads, cm
R	—	Gas constant, 8.314 J/mol K
R^2	—	Correlation coefficient
R_L	—	Separation factor
T	—	Absolute temperature, K
t, t_b, t_s, t_r	—	Time, breakthrough time, saturation time, total time taken in FBC, min

$t_{0.5}$	– Time required for 50% adsorbate breakthrough time, min
U_0	– Linear velocity of inlet effluent, cm/min
V, V_{eff}	– Volume of effluent, volume of effluent treated, mL
β	– Activity coefficient related to biosorption mean free energy, mol ² /kJ ²
ε	– Polanyi potential
τ	– Time required for 50% adsorbate breakthrough time in Yoon–Nelson model, min
ρ_p	– Apparent density of the adsorbent, g/mL
ρ_b	– Bulk density, g/mL

References

- [1] S. Vishali, Studies on Treatability of Paint Industry Wastewater by Physical Methods, Dissertation, SRM University, India, 2015.
- [2] S. Vishali, P. Rashmi, R. Karthikeyan, Potential of environmental-friendly, agro-based material *Strychnos potatorum*, as an adsorbent in the treatment of paint industry effluent, *Desal. Wat. Treat.*, 57 (2016) 18326–18337.
- [3] S. Vishali, R. Karthikeyan, S. Prabhakar, Utilization of seafood processing waste, as an adsorbent, in the treatment of paint industry effluent using a fixed-bed column, *Desal. Wat. Treat.*, 66 (2017) 149–157.
- [4] B. Noureddine, K. Ouzaoui, M. Abdenouri, E.L. Mohammed, Makhfouk, Dried prickly pear cactus (*Opuntia ficus indica*) cladodes as a low-cost and eco friendly biosorbent for dyes removal from aqueous solutions, *J. Taiwan. Inst. Chem. Eng.*, 44 (2013) 52–60.
- [5] S. Vishali, R. Karthikeyan, Cactus *Opuntia (Ficus-Indica)*: an eco friendly alternative coagulant in the treatment of paint effluent, *Desal. Wat. Treat.*, 56 (2014) 1489–1497.
- [6] A. Diaz, N. Rincon, A. Escorihuela, N. Fernandez, E. Chacin, C.F. Forster, A preliminary evaluation of turbidity removal by natural coagulants indigenous to Venezuela, *Process Biochem.*, 35 (1999) 391–395.
- [7] M.V. Jadhav, Y.S. Mahajan, Assessment of feasibility of natural coagulants in turbidity removal and modeling of coagulation process, *Desal. Wat. Treat.*, 52 (2014) 5812–5821.
- [8] U.S. Carpinteyro, M. Vaca, L. Torres, Can vegetal biopolymers work as coagulant- flocculant aids in the treatment of high-load cosmetic industrial wastewaters?, *Water Air Soil Pollut.*, 223 (2012) 4925–4936.
- [9] M. Dakiky, A. Khamis, Manassra, Selective adsorption of chromium (VI) in industrial wastewater using low-cost abundantly available adsorbents, *Adv. Environ. Sci.*, 6 (2002) 533–540.
- [10] M. Patricia, C. Munoz, A.C. Chavez, Experimental binding of lead to a low cost on biosorbent: Nopal (*Opuntia streptacantha*), *Bioresour. Technol.*, 99 (2008) 211–217.
- [11] R. Kumar, M.A. Barakat, Decolorization of hazardous brilliant green from aqueous solution using binary oxidized cactus fruit peel, *Bioresour. Technol.*, 226 (2013) 377–383.
- [12] APHA, Standard Methods for the Examination of Waste and Wastewater, sixteenth edition, American Public Health Associations, New York, NY, 1995.
- [13] S. Gupta, B.V. Babu, Experimental investigations and theoretical modeling aspects in column studies for removal of Cr (VI) from aqueous solutions using activated tamarind seeds, *J. Water Res. Prot.*, 2 (2010) 706–716.
- [14] A.A. Ahmad, B.H. Hameed, Fixed bed adsorption of reactive azo dye onto granular activated carbon prepared from waste, *J. Hazard. Mater.*, 175 (2010) 298–303.
- [15] D. Monal, J.B. Kumar, M.F. Hassan, G. Nitin, A. Kumar, Fixed bed column of textile dye direct blue 86 by using a composite adsorbent, *Arch. Appl. Sci. Res.*, 4 (2012) 882–891.
- [16] J.T. Nwabanne, P.K. Igbokwe, Adsorption of packed bed column for the removal of lead (II) using oil palm fibre, *Int. J. Appl. Sci. Eng.*, 2 (2012) 106–115.
- [17] X. Luo, Z. Deng, X. Lin, C. Zhang, Fixed bed column study for Cu²⁺ removal from solution using expanding rice husk, *J. Hazard Mater.*, 187 (2011) 182–189.
- [18] Z.Z. Chowdhury, S.M. Zain, A.K. Rashid, R.F. Rafique, K. Khalid, Breakthrough curve analysis for column dynamics sorption of Mn (II) ions from wastewater by using *Mangostana garcinia* Peel-based granular activated carbon, *J. Chem.*, (2013) 1–8.
- [19] S. Xiao Feng, T. Imai, M. Sekine, H. Takaya, Y. Koichi, K. Ariyo, N.A. Shiori, Adsorption of phosphate using calcined Mg₃-Fe layered double hydroxides in a fixed bed column study, *J. Ind. Eng. Chem.*, 20 (2014) 3623–3630.
- [20] X. Lin, R. Li, Q. Wen, J. Wu, J. Fan, X. Jin, W. Qian, D. Liu, X. Chen, Y. Chen, J. Xie, J. Bai, H. Ying, Experimental and modeling studies on the sorption breakthrough behaviors of butanol from aqueous solution in affixed bed of KA-I resin, *Biotechnol. Bioprocess Eng.*, 18 (2013) 223–233.
- [21] Z. Saadi, R. Saadi, R. Fazaeli, Fixed-bed adsorption dynamics of Pb (II) adsorption from aqueous solution using nanostructured γ -alumina, *J. Nanostruct. Chem.*, 3 (2013) 1–8.
- [22] A.O. Okewale, K.A. Babayemi, A.P. Olalekan, Adsorption isotherms and kinetics models of starchy adsorbents on uptake of water from ethanol–water systems, *Int. J. Appl. Sci. Technol.*, 3 (2013) 35–42.
- [23] R.N.P. Teixeira, V.O.S. Neto, J.T. Oliveira, T.C. Oliveira, D.Q. Melo, M.A.A. Silva, R.F. Nascimento, Study on the use of roasted barley powder for adsorption of Cu²⁺ ions in batch experiments and in fixed bed columns, *Bioresources*, 8 (2013) 3556–3573.
- [24] M. Kapur, M.K. Mondal, Mass transfer and related phenomena for Cr (VI) adsorption from aqueous solutions onto *Mangifera indica* saw dust, chemical engineering saw dust, *Chem. Eng. J.*, 218 (2013) 138–146.
- [25] I.E. Hristova, Comparison of different kinetic models for adsorption of heavy metals onto activated carbon from apricot stones, *Bulg. Chem. Commun.*, 43 (2011) 370–377.
- [26] S.V. Dimitrova, Removal of lead (II) from aqueous solutions by blast-furnace metallurgical slags, *Indian J. Eng. Mater. Sci.*, 5 (1998) 89–193.
- [27] V.P. Vinod, T.S. Anirudhan, Adsorption behavior of basic dyes on the humic acid immobilized pillared clay, *Water Air Soil Pollut.*, 150 (2003) 193–217.
- [28] E.W. Bao, Y.H. Yong, X. Lei, P. Kang, Biosorption behavior of azo dye by inactive CMC immobilized *Aspergillus fumigatus* beads, *Bioresour. Technol.*, 99 (2008) 794–800.